WiWear: Wearable Sensing via Directional WiFi Energy Harvesting

Vu H. Tran, Archan Misra
Singapore Management University
Singapore
{hvtran.2014, archanm}@smu.edu.sg

Jie Xiong
University of Massachusetts at Amherst
Amherst, MA 01003, USA
jxiong@cs.umass.edu

Rajesh Krishna Balan
Singapore Management University
Singapore
rajesh@smu.edu.sg

Abstract—Energy harvesting, from a diverse set of modes such as light or motion, has been viewed as the key to developing batteryless sensing devices. In this paper, we develop the nascent idea of harvesting RF energy from WiFi transmissions, applying it to power a prototype wearable device that captures and transmits accelerometer sensor data. Our solution, *WiWear*, has two key innovations: 1) beamforming WiFi transmissions to significantly boost the energy that a receiver can harvest ∼2-3 meters away, and 2) smart zero-energy, triggering of inertial sensing, that allows intelligent duty-cycled operation of devices whose transient power consumption far exceeds what can be instantaneously harvested. We provide experimental validation, using both careful measurement studies as well as a controlled study with human participants, to show the viability of a custom-built *WiWear*-based wearable device, at least in office environments.

Index Terms—Batteryless, Wearable, Beamforming, Harvesting, RF

I. Introduction

Energy remains perhaps the greatest challenge in the pervasive deployment of either wearable devices for activity sensing (e.g. eating [1], smoking [2], or stress levels [3]) or embedded devices for environmental sensing (e.g., [4]). In particular, sensors such as accelerometers or gyroscopes simply consume too much energy to operate continuously without either a dedicated power source or a large battery. However, using battery power introduces two distinct disadvantages: (i) frequent recharging may simply be cumbersome or impractical–e.g., for wearable-based monitoring of elderly health at home; (ii) also, high-density storage batteries give rise to *leakage* concerns and hazards, especially when the sensors are deployed in volume and out of sight (e.g., in industrial IoT settings).

To overcome these disadvantages, many solutions using renewable energy harvesting capabilities have been proposed–such as ambient light [5], temperature gradients [6] and kinetic energy [7]. Each such technique is innovative, but has its own limitations–e.g., ambient light cannot be used for sensors mounted in poorly lit or occluded locations (e.g., in a dark warehouse or on occluded body locations).

In this paper, we investigate the practical feasibility of using WiFi-compatible packets transmitted by a multi-antenna WiFi AP (access point) to power a wearable device with a relatively *high-power sensor*–an accelerometer. Wireless charging, itself, is not novel, but current solutions require either close proximity (3-5cm) to the transmitting power source (near field wireless charging, e.g., the Qi [8] standard based on magnetic induction used by modern high-end phones, which also requires precise alignment between the transmitter and receiver), or can only charge ultra-low power passive RFID tags [9] at longer ranges (far field wireless charging). More recently, PoWiFi [10] has demonstrated the use of WiFi, using multiple channels simultaneously, to power an ultra-low power wearable (with a temperature or camera sensor), with low duty cycles, while Energy-Ball [11] has shown how a grid of ceiling-mounted transmitters (working at 915MHz, whose propagation loss is much lower than the 2.4GHz WiFi channel) can collaboratively deliver high wireless power to such tags.

Our key scientific contributions are two-fold: we show (a) how to increase the harvested WiFi power (via directional WiFi transmissions) to much higher levels ($O(100\mu W)$), even on a single channel, on an embedded device, at a much greater distance (deliver over $30\mu W$ at ∼3meters from the transmitter) than had been previously possible. This facilitates many more use cases, in industrial IoT and smart homes/offices; and (b) that, with novel triggered-sensing techniques (extending the paradigm articulated in [12]), we can perform continual gesture tracking from a batteryless, accelerometer-equipped, wearable sensing device.

Our solution, called *WiWear*[1] uses beam-formed transmissions, by a multi-antenna AP, of WiFi "power packets" (transmissions performed explicitly to transfer RF energy) to deliver bursts of directed WiFi energy to a client device. To point the beam towards the client, *WiWear* utilizes AoA (angle-of-arrival) estimation techniques [14]. These AP-side techniques are paired with novel energy-conserving features on the wearable device, which activates its communication and sensing components intelligently and selectively, to help capture only key events.

Key Contributions: To our knowledge, we are the first to design and empirically demonstrate a working prototype (called *WiWear*) that uses WiFi transmissions, on a single WiFi channel, from one *realistically-distant* AP to power a batteryless, wrist-mounted wearable sensor device (which

---

[1]An initial vision was articulated in our preliminary work [13]. This paper, however, designs, implements and evaluates a fully-working WiFi based system.

collects significant accelerometer data). To achieve this goal, we make the following key contributions:

- *Use of Beamformed WiFi Transmissions for Power Delivery:* Through empirical experiments, it is clear that the harvested power, from a conventional omni-directionally transmitting WiFi AP, is too low for practical use: around $1 - 3\mu W$ at distances of 3-4 meters. To tackle this problem, we propose to leverage on prior work on AoA estimation and beamforming to spatially concentrate the transmitted power. Via experimental studies, we show that we can effectively perform AoA estimation with errors usually less than 5°and achieve an over *100-fold* increase in harvested power.

- *Design & Implementation of an Intermittently-Triggered Wearable:* We built a wrist-worn wearable device, which utilizes WiFi harvesting to power a *relatively high-power* inertial sensor used in various gesture-tracking applications. Such a wearable device, worn by a mobile user, gives rise to two challenges: (i) the WiFi AP must be able to track the wearable's changing location, without requiring constant active transmissions from the wearable, and (ii) the peak power overhead of the wearable system, including the accelerometer and the RF frontend, is over 40 mW– while low, this is much higher than the $O(100)\mu W$ harvested power to permit continuous sensing. To tackle both these challenges, the wearable employs a simple magnetic field tracker to first detect *significant motion* of the wearable device. Such significant motion triggers both (i) the transmission of "ping" packets, which allows the AP to determine the wearable's new AoA, and (ii) the activation of the accelerometer sensor, during the likely occurrence of meaningful gestures. A supercapacitor helps store the harvested RF energy, and smoothen out transient fluctuations in power supply and drainage.

- *Experimental Demonstration of* WiWear*:* By combining controlled & real-world studies with numerical analysis, we show the viability of *WiWear*. In particular, microstudies with a static wearable show that the wearable can harvest over 400 μW, at a distance of 1 meter. The harvested power remains high (over $30\mu W$) even at a distance of 3 meters. More importantly, we use a 4-person study in an office cubicle setting to show that *WiWear* can be used to *continuously* monitor for *major* hand movements, while being net energy-positive. Moreover, via numerical analysis, we show that, by appropriately adapting the spatial & temporal pattern of the RF beams, our AP can support multiple such wearables simultaneously.

We believe that our work lays the foundation of a practical WiFi-based energy harvesting mechanism for future higher-power wearable sensing devices, especially in AP-rich home & office environments.

II. Related Work

There has been a wide variety of related work in the broad areas of energy harvesting, including WiFi/RF energy harvesting, low-power wearable design, and WiFi beamforming.

A. Energy Harvesting for Client Devices

There is significant prior work on energy harvesting for wearable / embedded devices using light, kinetic energy, thermal gradients etc. Ambient and solar lighting generally provides the highest amount of harvested power as demonstrated by Heliomotes [15] to power embedded devices and Hande et. al [5] to power indoor APs. Kinetic energy is another popular energy harvesting source that can use body movements (e.g. EnergyBug [7]) and walking (e.g. SolePower [16]) to power ultra-low-power body sensors. Thermal energy harvesting (e.g., Thermes [4] and [17]) uses temperature gradients to generate an electrical charge. More recent work, such as Flicker [18], provide a platform for rapid prototyping of energy harvesting-based sensors. Our work is complementary to these prior methods and can be (a) used to operate higher power devices, and b) deployed in environments (e.g. dark warehouses) where prior methods would not work.

B. WiFi & RF harvesting

Harvesting power from wireless transmissions has also been studied and usually requires custom-designed hardware for the goal of charging RFID tags and devices – with WISP [19] being a very well known example that is used to power a variety of sensors. PoWiFi [10] is the work closest in spirit, and the precursor, to our approach. PoWiFi modifies AP firmware to transmit 'power packets' (without beamforming) on multiple free channels simultaneously, and harvests such RF energy, across multiple channels, using a matched filter on the receiver. Such WiFi power harvesting is used to operate low power embedded sensors at distances of up to 20ft, but with relatively low duty cycles (e.g., a camera image once every 20 mins). Most recently, PowerBall [11] has utilized careful phase synchronization across a large number (≈ 20) ceiling-mounted RF transmitters to deliver wireless power to specific locations, enabling the harvesting of around $600\mu W$ by *static* receivers within a 20X20m^2 area. Using beamforming to increase energy harvesting has been studied via simulations by Huang et. al [20] and Liu et. al [21]. We believe that *WiWear* is the first prototype to utilize directional WiFi transmissions from a single AP, together with a motion-triggered wearable sensing platform, to support human activity sensing.

C. WiFi-based Localization

WiWear requires accurate tracking of a wearable, potentially mobile, device, to perform accurate beamforming to relieve sufficient RF energy. Prior work, such as ArrayTrack [14] and Chronos [22] have shown how to leverage active client RF transmissions, coupled with precise AoA computations to very precisely locate the client. We use similar methods in *WiWear*. Device-free localization approaches, such as WiSee [23], and single AP methods, such as Bharadia et. al [24], Jain et. al [25], and IndoTrack [26] were also considered. But they are not robust enough for deployment in environments with multiple human occupants.
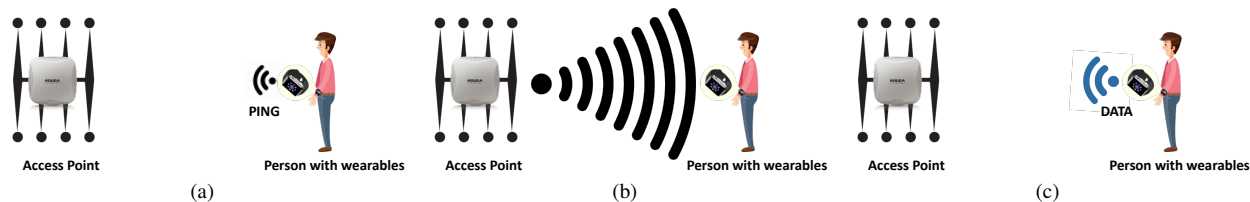
Fig. 1. 5-step model of *WiWear* architecture. a) Step1: The wearable sends a ping packet when triggered by gestures. Step2: The AP receives ping packets and estimates AoA of the device. b) Step3: The AP sends beamformed energy packets toward the device. Step4: The device harvests the energy from energy packets and stores it in a super-capacitor. c) Step5: the device uses the harvested energy to record sensory data, store it locally and transmit the data back to the server once available.

III. SYSTEM OVERVIEW

In this section, we present the overall functional architecture of *WiWear*, detailing the various system-level components needed to deliver sufficiently high WiFi-based energy to stationary or mobile devices. (The detailed design of the *WiWear* wearable and AP is described later, in Sections IV and V.)

Figure 1 shows the overall flow of *WiWear*. In this system, the wearable or embedded device (the 'client') transmits an omni-directional 'ping' message when triggered by significant hand movements (Step 1). A WiFi AP computes the AoA (angle of arrival) of such a 'ping' message and thereby establishes the client's relative angular orientation (Step 2). The WiFi AP then transmits *electronic beamformed* energy packets, delivering a more concentrated dose of RF energy towards the client device (Step 3). The client device utilizes a passive RF energy-harvesting circuit to convert this RF energy into an electrical current, storing the resulting energy in a super-capacitor (Step 4). This supercapacitor thus acts as a nano-battery, providing the transient power needed to activate the client's sensing (an accelerometer in our implementation) and communication modules when needed (Step 5). We shall see that the harvested RF energy, while two-orders of magnitude higher than prior systems, is still insufficient to power the (sensing, communication) modules continuously. Accordingly, the client device (a wrist-worn "wearable" prototype in our implementation) must employ a set of smart *activation* strategies, turning on its sensing and communication components intermittently.

A. Beamforming Technique

With the adoption of MIMO technologies in the latest 802.11n and 802.11ac WiFi standards, WiFi APs on the market are now equipped with multiple antennas: 4-antenna APs are quite commonplace, with 6&8 antenna products also becoming increasingly available[2]. The availability of such an antenna array provides us an opportunity to perform beamforming to achieve significantly more efficient power transfer. Beamforming, which is traditionally used to improve the reliability of data transfer, involves the careful control of the amplitude and phase of each antenna's transmission, so that they constructively add up in the target direction. The *beamwidth* is closely related to the number of antennas employed for beamforming:

[2]For example, the Aruba 320 series APs (http://www.arubanetworks.com/assets/ds/DS_AP320Series.pdf)

theoretically, the larger number of antennas, the thinner the beam we can achieve and thus, higher the concentration of RF power at a specific location. (Figure 2 shows the beamwidths obtained in our lab, using 4 and 8 antenna arrays.)
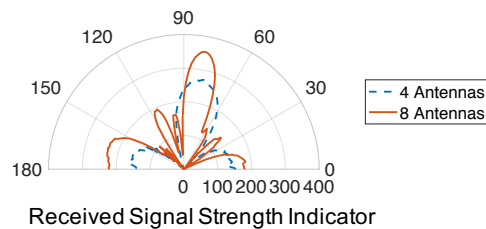

Fig. 2. Beamwidth Observed in Practice (4—8 Antenna Array)

B. Locating the Client Device

For beamformed energy transfer to be effective, the WiFi AP needs to know the location of the client device–more specifically, the *angular direction* of the client, *relative to the AP's own location*. To compute this, the WiFi AP utilizes its antenna array to determine the AoA of any wireless transmissions from the client device. The key principle for such angle/direction estimation is that the same signal propagates different amounts of distances to reach, and thus results in slight changes in the signal phase across, different antenna elements. We employ the state-of-the-art MUSIC algorithm [27] (which has been shown in [14] to estimate AoA with errors $\leq 10 - 15°$) to perform such AoA estimation. Note also that such AoA estimation is needed only when mobile/wearable devices *move*; it is unnecessary for scenarios where the devices are static.

C. Transmission & Sensing on the Client

Each client device harvests the transmitted RF energy, stores it to cover transient demand and utilizes such stored energy to perform its necessary sensing and communication tasks. The client transfers such data only periodically (using energy-efficient bursts) to the backend/cloud infrastructure. Given this periodic mode of operation, we do not currently envisage using *WiWear* to support applications that require real-time sensing and response. Moreover, the need to make the client device (e.g., the wrist-worn wearable) simple and cheap implies that the client's transmissions are omni-directional. The client transmissions have two distinct uses: (i) to transfer the collected sensor data to the backend, and (ii) to provide the 'ping' packets needed by the AP to estimate the client's directionality.
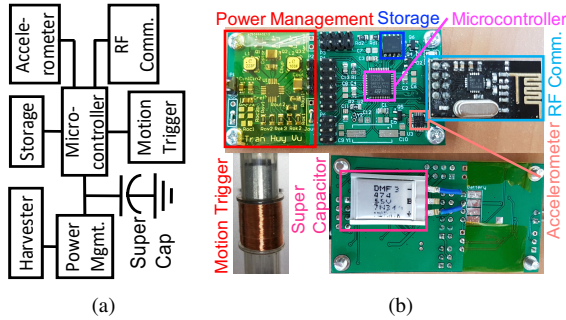
Fig. 3. a) Component-level diagram. b) Wearable Implementation.

IV. THE *WiWear* CLIENT DEVICE

We now describe the design & implementation of our RF energy harvesting based wearable device, which includes an accelerometer sensor that can help track an individual's movement and gestures. Figure 3a illustrates the overall component-level design of the wearable device, which contains a few key components: an RF-energy harvester, a low-power microcontroller, the low-power accelerometer sensor, a storage unit, a wireless communication interface, a supercapacitor (to provide transient energy storage) and a power management module. Figure 3b shows the implementation on a PCB.

1) The RF Energy Harvester: The RF harvester works by converting the received wireless transmissions into an output voltage. In our current effort, we do not focus on developing the "best harvester", but instead on demonstrating the overall viability of *WiWear*. Accordingly, we implement the harvester (illustrated in Figure 4) on a commonplace prototype PCB (FR4 material). The harvester includes an LC network, followed by a rectifier. We hand-tune the inductor (approximately 1 round of wire) until the resonant voltage is highest on the WiFi 802.11b channel 1 (the channel used by the WiFi AP for transmitting "power packets" in our study). However, the instantaneous output voltage usually fluctuates significantly with slight movements of the wearable, implying that it is not stable enough to operate the wearable directly. We use a boost converter, BQ25570, which stores low voltage energy (as low as 100mV) and boosts it into a higher programmable voltage (set to 2.57V in our implementation) for common electronic devices. This output voltage is then used to operate an entire embedded system including 1 microcontroller, 1 inertial sensor, and 1 RF communication front-end.
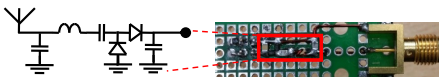

Fig. 4. RF Harvester: FR4 PCB & hand-tuned inductor.

2) The Microcontroller+ Sensor: We utilize a commodity low-power microcontroller, the STM32L053 [28], which consumes 6.6 mW power at normal operation, but only 1 μW power during stop mode. In stop mode, all functions of the device are stopped, but the content of RAM is preserved. In our system, when the accelerometer records enough data, it generates an interrupt signal to wake up the microcontroller to

read the buffer. The microcontroller wakes up every 3 seconds to read 90 bytes of acceleration data from the accelerometer if the accelerometer is actually active. The wearable can store the acceleration data in a FRAM storage unit, the Cypress FM25VN10, (for a transmission burst later) or transmit the data back to the server using the RF front-end. Our device implementation uses the LIS3DHTR 3-axis accelerometer from STMicroelectronics. This low-power sensor consumes 2 μA at 1 Hz, and 6 μA at 50 Hz. According to [29], 98% of frequency spectrum power of accelerometer signals for human activities such as walking lies under 10 Hz. Accordingly, we use a sampling frequency of 10 Hz, as this proves adequate in tracking most natural gestures (in addition, gesture recognition approaches often filter out high-frequency noise).
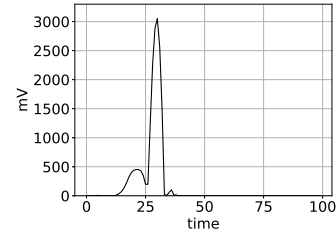

Fig. 5. Voltage generated by motion trigger.

3) Zero-Energy Motion Trigger: To minimize the unnecessary energy drain of the wearable device, we adopt a triggering-based mechanism, whereby the sensor and the microcontroller are activated only *when the wearable device experiences significant motion* (e.g., when the user makes a gesture). To avoid the energy drain from such motion monitoring, we include a very simple, "zero-energy", passive, motion trigger: a coil (taken from a shake torch) with a Neodymium magnet inside. Whenever the device is subject to a significant movement, the coil generates a voltage high enough (see Figure 5) to trigger an external interrupt to the microcontroller, which then activates the rest of the components. This trigger also causes the controller to generate and send out 'ping' packets, which the AP can then use to infer the client's updated AoA. Our motion trigger component is more sensitive to rotational movements but less sensitive to subtle linear motion. However, this was not a limitation in our current studies (in an office meeting room), where user gestures typically include a sufficient rotational component. There are prior studies on tiny MEMS-based motion energy harvesters [30], [31] that may provide greater linear and rotational motion sensitivity—we shall explore these in future work.

V. THE *WiWear* AP

We now describe the design and implementation of our enhanced WiFi AP. To support the beamforming-based RF charging vision, the AP needs to perform the following additional functions: (i) detection of the 'ping' packets; (ii) determination of the AoA and (iii) beamformed transmission of 'power' packets. We implemented our functionality using the WARP [32] platform, which is widely used within the research community. By default, each WARP board can

support a maximum of 4 antennas. To support more precise beamforming using an 8-antenna AP, we coupled the operation of 2 separate WARP boards (Figure 7). To enable beamforming and AoA estimation, the phase difference among the antennas (across the two boards) must be precisely calibrated, and they must capture or transmit data at *exactly* the same time. We use a CM-PLL cable to synchronize the operation of the two boards, setting one board as a master to perform all the functions of a regular 802.11 AP. The second board performs as a slave, receives packets (for transmission) via the Ethernet interface and transmitting them wirelessly when triggered by the master. To support dynamic beamforming of power packets, we insert a complex multiplier at each antenna interface whose coefficients are specified within the power packet. Though the transceivers on the WARP board support both 2.4 GHz and 5 GHz band, the reference design supports only 2.4 GHz. In newer APs, one may conceivably use the 2.4 GHz band for energy and the 5 GHz band for usual data communication. Operating in a higher frequency band (e.g., 5 GHz) involves a tradeoff between higher path-loss, but greater possible number of antenna elements (providing narrower beams)–such studies are deferred to future work.

A. Detection of Low-power GFSK 'Ping' Packets

The *WiWear* wearable uses a low power NRF24L01+ module to transmit the 'ping' packets, whenever it is subject to a significant movement. This RF module uses GFSK modulation with a maximum 2Mbps data rate. The preamble of each packet is merely 8-bits ("01010101") followed by a 3-5 byte address. This makes the packet detection by the AP much more challenging compared to usual WiFi packet detection for 2 reasons: 1) These packets are not WiFi compatible. The preamble is too short compared with a usual WiFi preamble (hundreds of symbols). 2) The signal is too narrow band, with each packet preceded by 1.5 cycles of very low frequency ($\sim$40 KHz) while the RSSI circuit in the transceiver computes the RSSI across the whole range of 20MHz bandwidth. This produces very low and unstable RSSI readings of 'ping' packets at the WARP, which must support the wider 20 MHz band of WiFi and thus generates incorrect gain values from its Automatic Gain Control (AGC). We tackle this problem by using the frequency overlap between consecutive WiFi channels (consecutive channels have 15MHz overlap, the space between the 2 center frequencies is 5MHz): the wearable transmits such packets at the next higher channel, while the WARP board is tuned to the lower channel (see Figure 6). Specifically, in our current settings, the RF device transmits at channel 2 (center frequency at 2417MHz) while the WARP AP uses channel 1 (center frequency at 2412MHz). As a consequence of the resulting 5 MHz shift between the transmission and reception center frequencies, the received signal bandwidth becomes wider because 5MHz will be automatically added to the original GFSK signal (Figure 6b, the top plot). Therefore the transceiver on the WARP board produces a significantly more stable signal. The receiver (AP) then needs to remove the 5MHz from the received signal to restore the original narrow-band GFSK signal (Figure 6b, the middle plot). Figure 6 also shows that the received signal using overlap channel is less affected by DC offset.
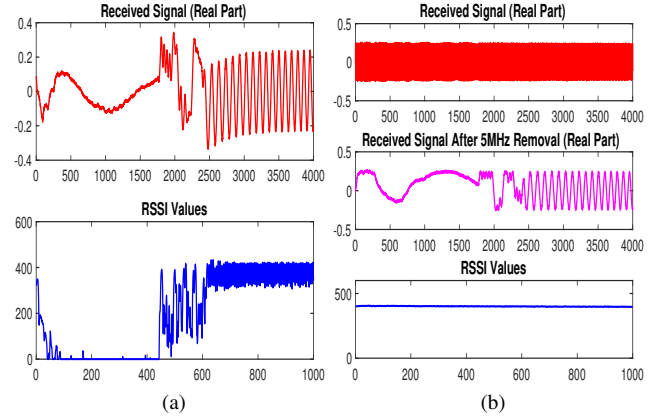

Fig. 6. a) Received signal and RSSI values from nRF24L01+ device and corresponding RSSI recorded at the same channel. The RSSI is unstable and some parts become zeros. DC offset is also observed. b) Received signal of another packet (before and after applying -5MHz shift) and RSSI values using channel overlap. Much more stable signal is observed with almost no DC offset.
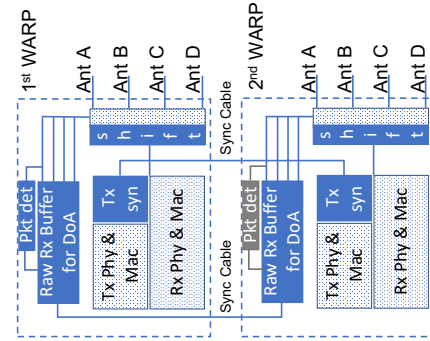

Fig. 7. AP Modification for beamforming and AoA. The dark blue parts are our extension.

B. Extension for AoA Estimation

The default 802.11 reference design in WARP board supports only 1 receiver path, though the system can switch among either its 4 antennas. As AoA estimation requires simultaneously data capture from multiple antennas concurrently, we modified the design to add a circular buffer. This buffer stores the data from all 4 antennas whenever a packet (from a wearable) is detected, and can also store similar data from the 4 antennas on the slave WARP board. A control server then reads the packets in the buffers to estimate the AoA of incoming packets.

C. Extension for Beamforming

To support the per-antenna phase control needed for beamformed transmission, We insert a complex multiplier (whose coefficient can be controlled through a register) to each antenna output. This allows the dynamic change of the phase of any transmitted packets before it is transferred. We also add to overcome an additional challenge, in ensuring concurrency

when the two WARP boards are used concurrently. If each WARP operated as an independent AP, their transmission schedules could differ, due to differences in their underlying carrier sensing. To overcome this, we disable the MAC layer of the slave board so that it will transmit a packet as soon as the master sends it a 'transmit' signal.

D. Beamforming with Multiple Clients

The AP behavior has thus far been defined in terms of beamforming for a single wearable device. When multiple client devices are present, an AP can judiciously either time-multiplex its power packet transmissions to different devices, or adjust its beamwidth (e.g., creating two separate 4-antenna beams) to simultaneously cover multiple devices, albeit with lower harvesting power/device. Such multi-device environments require the WiFI AP to optimize its operations carefully considering coverage vs. energy density tradeoffs (as a function of beamwidth), similar to the prior exploration of rate—throughput—coverage tradeoffs in broadcast wireless networks [33], [34].

Our current AP utilizes an optimization algorithm to choose between such beam shaping and/or time multiplexing choices. Conceptually, we divide the antenna array into K subarrays of size N, k^{th} subarray can point to direction $\Phi_k, k = 0..K-1$, and seek to determine the pointing direction of each subarray so that the energy objective is maximized. We consider 2 different objective functions: (a) maximize the total energy harvested (Max-Sum) and (b) maximize the minimum harvested energy, across the devices (Max-Min). The second objective promotes fairness by ensuring that no individual device "starves" of energy.

For Uniform Linear Array (ULA), the phase of the kth subarray (and thus its pointing direction) is adjusted by adjusting the phase of each of its antennas in a linear fashion according to: $Phase(Antenna_k^n) = (K \times N + n) \times \Phi_k, n = 0..N-1$. Using this assignment, each sub-array forms one beam separately; however, if two sub-arrays point to the same direction, they effectively form a narrower single beam. Given such a set of input directions $\{\Phi_k\}$, we use Matlab's Phased Array ToolBox to pre-compute a Look-Up-Table (LUT) to compute the collective response: $LUT(\Phi_0, \Phi_1, ..., \Phi_{K-1}) = response(\Phi_0, \Phi_1, ..., \Phi_{K-1})$ for any given angular direction. Hence, the angle-selection problem becomes (θ_i is the angle of ith device):

Max-Sum : $argmax(\Sigma_{i=0..M-1}LUT(\Phi_0, \Phi_1, ..., \Phi_{K-1})[\theta_i])$;

Max-Min : $argmax(\min_{i=0..M-1} LUT(\Phi_0, \Phi_1, ..., \Phi_{K-1})[\theta_i])$;

Figure 8 plots the simulated values for harvested power for a 2-user scenario (the technique is extensible to more devices), as a function of the angular separation $\Delta(\theta)$ between the devices ($\Delta(\theta)$=0°for collocated users). As a single ULA can estimate only orientation but not distance, we assume the devices are equi-distant from the antenna array and thus use the antenna response as a proxy for harvested signal power. Figure 8a shows the synthesized beam pattern for 2

methods when $\Delta(\theta) = 60°$: 2 concurrent 4-antenna beams and a single time-multiplexed 8-antenna beam. Similarly, Figure 8b shows the total relative power, received by 2 devices using 3 proposed methods: Max-sum, Max-min and Time-multiplexing. Under wider angular separation, Max-sum results in larger total power, but one or more devices can starve. In general, we see that concurrent beamforming outperforms the time-multiplexing of a single 8-antenna beam. The perform illustrated here can be enhanced further: e.g., using multi-AP triangulation [14] to estimate distance or weighting the utility function to capture differential power demands of different devices.
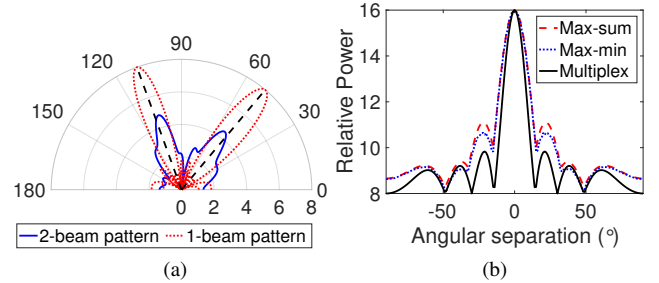

Fig. 8. a) Beam shaping: two beams and one beam ($\Delta(\theta) = 60°$) b) Total relative power (for different metrics,strategies)

VI. PERFORMANCE EVALUATION: MICRO-BENCHMARKS

In this section, we shall study how *WiWear* works under *controlled* conditions–i.e., when the *WiWear* wearable platform is stationary, and not mounted on any real user. These micro studies help establish the performance characteristics of each individual component (e.g., AoA determination, beamformed energy harvesting) and the resulting impact on the harvester energy output, under different conditions.
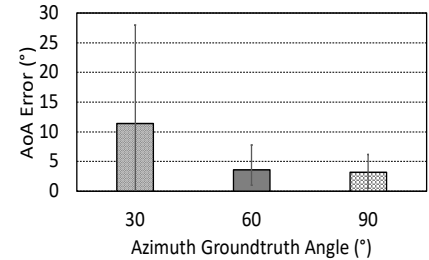

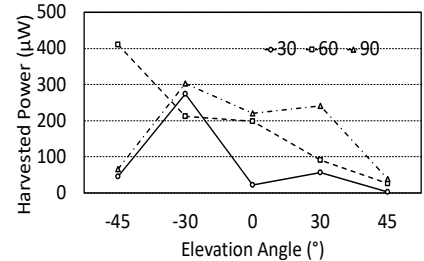Fig. 9. AoA estimation error at different azimuth angles.

Fig. 10. Harvested energy at different azimuth and elevation angles.

A. Experiment Setup & Calibration

All our experiments were conducted in a meeting room (3.5m x 4.5m) of our university building. The WARP system was installed on a table (1.1m x 1.9m) in the middle of the room–Figure 12 (shown later) demonstrates the setup used. For these studies, we use the same wearable device used in user studies (Section VII), but we do not connect the harvester's output to the power management unit of the wearable device. The AP transmits standard 802.11 packets with different power levels, but it transmits power packets at maximum power (20dBm) per antenna; thus, *in all experiments, our total transmitted power was well within the EIRP upper bound of 800mW*. A software program running on a computer generates 1024-byte 'power' packets (UDP packets with phase coefficients of 8 antennas) *continuously* (except for the study in Section VI, where we intentionally varied the percentage of 'power' packets). We place the wearable device on a tripod. For each study setting, we manually trigger the wearable device to transmit 'ping' packets, such that the AP can update its beam to point in the estimated direction of the wearable. We then record the average power of the harvester output with a 10kOhm resistive load.

B. Change in Azimuthal Orientation

We investigate the performance of the system (both AoA and Energy Beamforming) under different angles, with the wearable placed 1 meter from the AP. In theory, the performance of the system from $0°$ to $90°$ should be similar to $180°$ to $90°$ (the front half of the *azimuth* plane). However, the beam intensity in the space below and above the antennas (i.e., for different values of the *elevation*) should be different. We measure the system performance with 3 different azimuth angles $\{30°, 60°, 90°\}$ and 5 different elevation angles at $\{-45°, -30°, 0°, 30°, 45°\}$.

Figure 9 shows the AoA estimation error for different azimuth and elevation angles. It is known that the MUSIC algorithm becomes inaccurate as the azimuth angle approaches $0°$ or $180°$. Indeed, we see that the AoA error is $\leq 5°$ when the azimuth angle $\leq 60°$, but reaches a median value of $12°$, when the azimuth is $30°$. However, $120°$ ($30°$ to $150°$) is indeed an unnaturally wide field of view for practical scenarios. Figure 10 shows the harvested energy accordingly. The results suggest that the harvested energy remains fairly high as the elevation angle from $-30°$ to $30°$. In our office room setting, the AP is able to cover almost the entire room with an elevation angle of $30°$ and azimuth of $60°$; within this space, the harvester is able to harness over $200~\mu W$.

C. Energy harvesting vs. Distance

We next study how the efficiency of energy transfer diminishes with an increasing AP-wearable distance. Figure 11a shows the harvested energy, as the distance is varied from 1m-3m., with (azimuth=$90°$, elevation=$0°$). The results show that, even at 3m, the AP can still transfer about $33\mu W$ to the harvester. Given that our wearable with drains out only $23\mu W$ (from the built-in $220\mu F$ supercapacitor) even when it

is continuously recording the accelerometer reading (without transmitting 'ping' packets), we see that *our paradigm of beam-formed WiFi energy transfer is able to support the uninterrupted operation of the* WiWear *wearable essentially **anywhere** within a standard meeting room*.

D. Energy harvesting vs. Background data

We next study how the energy transfer efficiency is affected by the need for the AP's power packet transmissions to co-exist with regular WiFi data packets. Note that our modified AP implements the 802.11 AP reference design (from MangoComm [35]), and is thus able to provide data connectivity to regular WiFi clients. We study the sensitivity of efficiency by varying the percentage of broadcasted IP (data) packets & power packets. Figure 11b shows that the harvested energy decreases quite linearly with the percentage of IP packets. When the AP exclusively transmits IP packets (100%), the harvested power is almost zero as the AP transmits such packets using only 1 antenna and usually at less than the highest permitted power level. At the typical utilization (20%) observed on our campus WiFi network, *WiWear* appears to be capable of harvesting $200\mu W$, a 100-fold increase from ambient power levels.

E. Effect of Number of Antennas

We next vary the number of transmitting antennas in the WARP transmitter and study the impact on the harvested power (wearable-AP distance= 1 meter). Figure 11c plots the harvested power. Matching our intuition, a larger number of antennas allows the transmission beamwidth to be thinner, thereby effectively increasing the density of the delivered RF power. Interestingly, we observe that the angle at which the harvester gets the maximum energy differs a bit from the ground-truth, with the difference increasing from $5°$ to $20°$, when the number of antennas is reduced from 8 to 2, respectively. We suspect that this is due to the inevitable errors in phase control, with the phase errors getting averaged out when the number of antennas is higher. However, in practical environments, an overly thin beam may be counterproductive as errors in AoA estimation (especially in more crowded environments) may cause the narrow RF beam to be misdirected, resulting in a very sharp drop in the power harvested.

VII. CONSTRAINED USER STUDIES

We now evaluate the performance of the *WiWear* prototype, under constrained user studies performed in our 3.5m x 4.5m meeting room, set up to mimic a typical work environment. "Constrained" refers to the fact that the users are requested to stay within the meeting room during the study duration (30 minutes) and perform their "normal" office activities, while wearing the *WiWear* wearable device. Each user is, however, free to perform one or more activities of their choice (e.g., typing on a laptop, taking short breaks and stretching, etc.). Unlike Section VI, the wearable is now subject to human-specific movement and resultant changes to its performance
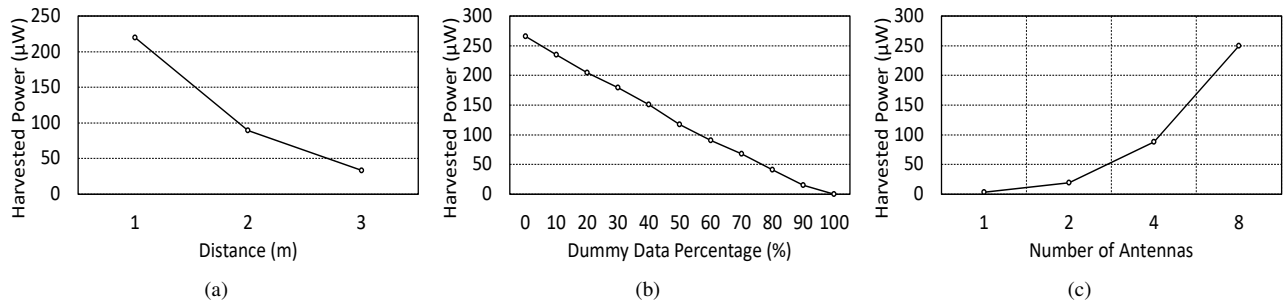
Fig. 11. a) Power vs. distance. b) Power vs. Varying 'data' traffic load c) Harvested Power vs. No. of Antennas.
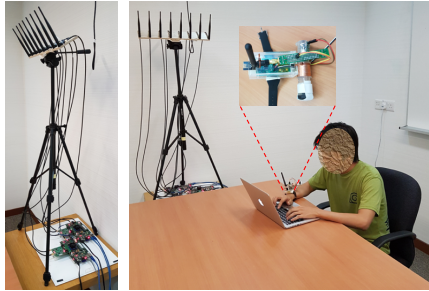

Fig. 12. Experimental Setup: (a) Left: The AP, comprising 2 WARP boards. (b) Right: A user wearing the *WiWear* device during the study.

metrics (e.g., AoA estimation error and fluctuations in harvested energy). As before, experiments are performed using an 8-antenna AP array, with the maximum total transmission output of 800mW, (*below the EIRP limit*).

We studied the behavior of 4 distinct users, each of whom was asked to initially sit at a different corner of our 1.1m x 1.9m table (see Figure 12) and subsequently perform their usual desk-based office chores for 30 minutes. The super-capacitor helps tide over the fluctuations in harvested power, caused due to such arm movements. We also experimented with smaller capacitors: Figure 14 shows the transient shortage of energy when using a small capacitor (10μF). Our studies revealed a trade-off: a larger (0.47F) capacitor can buffer enough energy for hours, but its leakage is higher ($\sim13\mu$W higher) than a smaller (220μF) capacitor, which can support the wearable operation for less than a minute. To deal with longer-lived periods of deficient harvesting (a user might cover his hands or move it to a blind spot for several minutes), we chose the 0.47F super-capacitor, which ensures that the available energy is never depleted during the experiment. The overall operation of the *WiWear* wearable is then as follows: The device usually sleeps, until the motion detector unit (the magnetic coil) triggers the wearable. The accelerometer is then activated, recording the acceleration values every 3 seconds over a 12-second interval. If a separate motion trigger is fired during this 12-second period, the activation time is extended again by 12 seconds. The wearable logs all the collected accelerometer data locally using a FRAM storage. At the end of the study episode, all the recorded samples are transmitted back to the AP and the voltage at the capacitor is measured. A comparison of the energy stored in the super-capacitor

before and after the experiment helps to determine if the overall harvested energy is sufficient (or not) to support the sensing, local storage and 'ping' packet transmission tasks. We compute the stored energy in a capacitor using the equation:

$$U = \frac{1}{2}CV^2; \quad P = \frac{\Delta U}{T}; \quad (1)$$

where C is the capacitance (=0.47F), V is the voltage in Volt, U is the stored energy in Joule, P is the 'average' power in Watt, and T is the observation duration (30 mins). In other words, P represents the power differential (averaged over 30 minutes) between the harvested and expended power.

As illustrated in Figure 12, the AP is placed behind the table, the 8 antennas are raised up to 0.9m and point down to the middle of the table (45°). Figure 13a plots the average differential power (the net change in super-capacitor energy, divided by 30 minutes) of each user. We observed differences in the activities performed by the 4 users: one user read paper-based text; one worked on his aluminum-bodied laptop (primarily reading content), while two used their smartphones. As expected, the device on two users located at the corners closest to the AP harvest the highest power and end up with the largest positive residual power.

However, the AoA estimation of the second user (see Figure 13b) is sometimes quite inaccurate (maximum error = 32°), in contrast to the other users whose error is usually $\leq 5°$. We suspect that the RF reflectivity of the laptop's aluminum body may be a contributory factor. Figure 13c shows the total duration for which each user's accelerometer data is recorded. We also notice that the user reading documents on a laptop (user 2) triggers the system less often than the user reading paper-based document (user 1), likely due to the greater hand motion involved in turning pages on a physical document. While the 3rd user (User 3) simply performs browsing on his smartphone, User 4 is much more active, resulting in the capture of over 4 minutes of his hand movement. Note that even though these users are located farthest from the AP (2.2m and 2m respectively), the wearable device still ends up being net-power positive.

Overall, our results demonstrate that the WiWear's *battery-less wearable can indeed continually monitor the key hand movements of users, as the harvested energy is greater than the expenditure in all 4 cases.* This energy-positive operation occurs even though our current linear antenna is known to
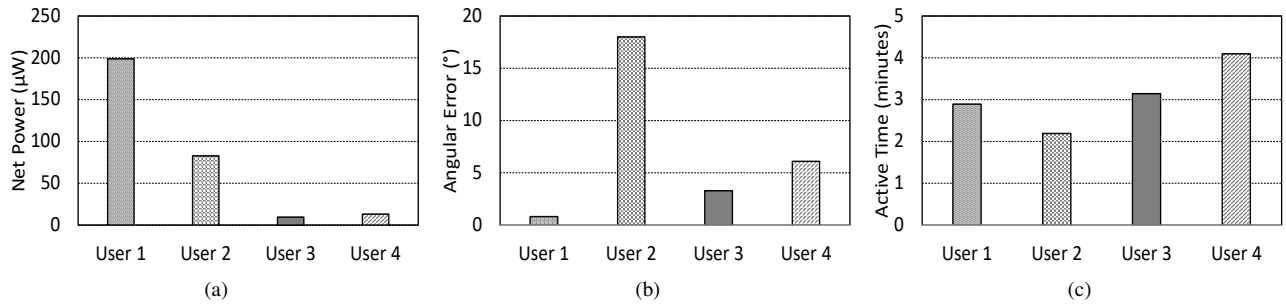
Fig. 13. a) Net energy for 4 users (distance = {1.3, 1.4, 2.2, 2} meters). b) AoA error (4 users). c) Active accelerometer sensing period.
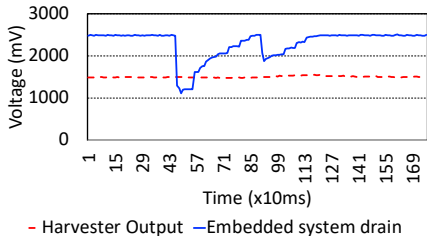

Fig. 14. Time series of wearable voltage using $10\mu F$ small capacitor.

have very low gain near its poles; the use of better antenna designs should further enhance the energy harvested.

VIII. DISCUSSION

While our results attest to the promise of *WiWear*, there are, however, several open issues to explore further.

Multi-AP Operation: In a practical campus or factory environment, multiple APs are likely to 'cover' a specific location (e.g., in our campus, the number of APs overheard at a typical location is 5-6). This opens up additional possibilities. Clearly, as illustrated in EnergyBall [11], transmission of suitably beamformed transmissions on a common channel, along with careful phase control, can significantly increase the harvested energy. Alternately, each AP can transmit its 'power packets' on its own independent channel, thereby eliminating the difficult task of phase synchronization. However, the RF harvester module on the wearable must be enhanced ([10]) to (a) allow the harvester to simultaneously support multiple resonant AP frequencies, and (b) implement dynamic impedance matching (e.g., [36]).

Power vs. Throughput Tradeoffs: Our early results (Section VI.D) show that there is a tradeoff between the two objectives of data transfer and RF charging that remains to be explored. Additional mechanisms may be used to optimize this tradeoff: e.g., adjusting the schedule & duty cycle of power packet transmissions (e.g., by using multiple virtual queues [37]) to avoid unacceptable loss or latency of data packets or transmitting data packets at higher power (for enhanced energy harvesting).

Additional & Improved Energy Harvesting: The current *WiWear* prototype uses a basic whip antenna for energy harvesting (gain=2.1 dBi), whose performance degrades for large values of either the azimuthal or elevation angles. It is very

likely that alternative antenna designs (e.g., a metallic strip-based "patch antenna) can increase the harvested energy significantly (see [38]). Moreover, wearables may combine WiFi energy harvesting with other alternative harvesting techniques, such as ambient light, for significantly improved performance. Also, the magnetic trigger may be replaced with a kinetic energy harvester (such as the ones used in mechanical watches) that also harvests additional energy.

Other Application Domains & Paradigms: Our investigations focused on a single AP, with a single user in an office-like setting. Additional research is needed to apply the core *WiWear* concept to other scenarios, such as (a) capturing key locomotion and gesture-related behaviors (e.g., fall detection) of elderly inhabitants in smart homes; (b) operating static sensors, deployed in industrial sites and warehouses.

IX. CONCLUSION

In this paper, we presented *WiWear*, an approach for batteryless sensing that uses beamforming of WiFi transmissions to enable a wearable receiver to harvest more than $400\mu W$ of energy at a distance of 1 meter, and more than $30\mu W$ even when the distance increases to 3 meters. *WiWear* couples this harvesting with smart event triggering, using a passive motion detector, to duty cycle a full accelerometer-equipped wearable device whose instantaneous power drain (including processor and wireless data interface) is more than 40 mW. Via measurements and user studies performed in a representative office setting, we see that *WiWear* can be a viable approach for batteryless sensing of gestures. We also identified open issues, which we are currently addressing to develop a more robust and widely-applicable *WiWear* prototype.

REFERENCES

[1] E. Thomaz, I. Essa, and G. D. Abowd, "A practical approach for recognizing eating moments with wrist-mounted inertial sensing," in *Proceedings of the 2015 ACM International Joint Conference on Pervasive and Ubiquitous Computing*, ser. UbiComp '15. ACM, 2015, pp. 1029–1040.

[2] A. Parate, M.-C. Chiu, C. Chadowitz, D. Ganesan, and E. Kalogerakis, "Risq: Recognizing smoking gestures with inertial sensors on a wristband," in *Proceedings of the 12th Annual International Conference on Mobile Systems, Applications, and Services*, ser. MobiSys '14. ACM, 2014, pp. 149–161.

[3] E. Ertin, N. Stohs, S. Kumar, A. Raij, M. al'Absi, and S. Shah, "Autosense: Unobtrusively wearable sensor suite for inferring the onset, causality, and consequences of stress in the field," in *Proceedings of the 9th ACM Conference on Embedded Networked Sensor Systems*, ser. SenSys '11. ACM, 2011, pp. 274–287.

[4] B. Campbell and P. Dutta, "An energy-harvesting sensor architecture and toolkit for building monitoring and event detection," in *Proceedings of the 1st ACM Conference on Embedded Systems for Energy-Efficient Buildings*, ser. BuildSys '14. ACM, 2014.

[5] A. Hande, T. Polk, W. Walker, and D. Bhatia, "Indoor solar energy harvesting for sensor network router nodes," *Microprocess. Microsyst.*, vol. 31, no. 6, Sep. 2007.

[6] B. Campbell, B. Ghena, and P. Dutta, "Energy-harvesting thermoelectric sensing for unobtrusive water and appliance metering," in *Proceedings of the 2Nd International Workshop on Energy Neutral Sensing Systems*, ser. ENSsys '14. ACM, 2014.

[7] K. Ryokai, P. Su, E. Kim, and B. Rollins, "Energybugs: Energy harvesting wearables for children," in *Proceedings of the SIGCHI Conference on Human Factors in Computing Systems*, ser. CHI '14. New York, NY, USA: ACM, 2014.

[8] X. Liu, "Qi standard wireless power transfer technology development toward spatial freedom," *IEEE Circuits and Systems Magazine*, vol. 15, no. 2, pp. 32–39, Secondquarter 2015.

[9] D. J. Yeager, P. S. Powledge, R. Prasad, D. Wetherall, and J. R. Smith, "Wirelessly-charged uhf tags for sensor data collection," in *2008 IEEE International Conference on RFID*, April 2008.

[10] V. Talla, B. Kellogg, B. Ransford, S. Naderiparizi, S. Gollakota, and J. R. Smith, "Powering the next billion devices with wi-fi," in *Proceedings of the 11th ACM Conference on Emerging Networking Experiments and Technologies*. ACM, 2015, p. 4.

[11] X. Fan, H. Ding, S. Li, M. Sanzari, Y. Zhang, W. Trappe, Z. Han, and R. E. Howard, "Energy-ball: Wireless power transfer for batteryless internet of things through distributed beamforming," *Proc. ACM Interact. Mob. Wearable Ubiquitous Technol.*, vol. 2, no. 2, Jul. 2018.

[12] J. Hester and J. Sorber, "The future of sensing is batteryless, intermittent, and awesome," in *Proceedings of the 15th ACM Conference on Embedded Network Sensor Systems*, ser. SenSys '17. ACM, 2017.

[13] V. H. Tran, A. Misra, J. Xiong, and N. Hirunima, "Can wifi beamforming support an energy-harvesting wearable?" in *Proceedings of the Fifth ACM International Workshop on Energy Harvesting and Energy-Neutral Sensing Systems*, ser. ENSsys'17. ACM, 2017.

[14] J. Xiong and K. Jamieson, "Arraytrack: A fine-grained indoor location system," in *10th Usenix Symposium on Networked Systems Design and Implementation*. USENIX, 2013.

[15] K. Lin, J. Yu, J. Hsu, S. Zahedi, D. Lee, J. Friedman, A. Kansal, V. Raghunathan, and M. Srivastava, "Heliomote: Enabling long-lived sensor networks through solar energy harvesting," in *Proceedings of the 3rd International Conference on Embedded Networked Sensor Systems*, ser. SenSys '05. ACM, 2005.

[16] "Solepower smart boots," http://www.solepowertech.com/smartboots/, 2018, accessed: 2018-04-04.

[17] G. Xu, Y. Yang, Y. Zhou, and J. Liu, "Wearable thermal energy harvester powered by human foot," *Frontiers in Energy*, vol. 7, no. 1, 2013.

[18] J. Hester and J. Sorber, "Flicker: Rapid prototyping for the batteryless internet-of-things," in *Proceedings of the 15th ACM Conference on Embedded Network Sensor Systems*, ser. SenSys '17. ACM, 2017.

[19] A. P. Sample, D. J. Yeager, P. S. Powledge, A. V. Mamishev, and J. R. Smith, "Design of an rfid-based battery-free programmable sensing platform," *IEEE Transactions on Instrumentation and Measurement*, vol. 57, no. 11, pp. 2608–2615, Nov 2008.

[20] W. Huang, H. Chen, Y. Li, and B. Vucetic, "On the performance of multi-antenna wireless-powered communications with energy beamforming," *IEEE Transactions on Vehicular Technology*, vol. 65, no. 3, pp. 1801–1808, 2016.

[21] L. Liu, R. Zhang, and K.-C. Chua, "Multi-antenna wireless powered communication with energy beamforming," *IEEE Transactions on Communications*, vol. 62, no. 12, pp. 4349–4361, 2014.

[22] D. Vasisht, S. Kumar, and D. Katabi, "Decimeter-level localization with a single wifi access point," in *Proceedings of the 13th Usenix Conference on Networked Systems Design and Implementation*, ser. NSDI'16. USENIX Association, 2016, pp. 165–178.

[23] Q. Pu, S. Gupta, S. Gollakota, and S. Patel, "Whole-home gesture recognition using wireless signals," in *Proceedings of the 19th annual international conference on Mobile computing & networking*. ACM, 2013, pp. 27–38.

[24] D. Bharadia, E. McMilin, and S. Katti, "Full duplex radios," in *ACM SIGCOMM Computer Communication Review*, vol. 43, no. 4. ACM, 2013, pp. 375–386.

[25] M. Jain, J. I. Choi, T. Kim, D. Bharadia, S. Seth, K. Srinivasan, P. Levis, S. Katti, and P. Sinha, "Practical, real-time, full duplex wireless," in *Proceedings of the 17th annual international conference on Mobile computing and networking*. ACM, 2011, pp. 301–312.

[26] X. Li, D. Zhang, Q. Lv, J. Xiong, S. Li, Y. Zhang, and H. Mei, "Indotrack: Device-free indoor human tracking with commodity wi-fi," *Proc. ACM Interact. Mob. Wearable Ubiquitous Technol.*, vol. 1, no. 3, Sep. 2017.

[27] R. Schmidt, "Multiple emitter location and signal parameter estimation," *IEEE transactions on antennas and propagation*, vol. 34, no. 3, pp. 276–280, 1986.

[28] "Ultra-low-power arm cortex-m0+ mcu with 64 kbytes flash, 32 mhz cpu, usb, lcd," http://www.st.com/en/microcontrollers/stm32l053r8.html, 2018, accessed: 2018-04-08.

[29] E. K. Antonsson and R. W. Mann, "The frequency content of gait," *Journal of biomechanics*, vol. 18, no. 1, pp. 39–47, 1985.

[30] P. Miao, P. Mitcheson, A. Holmes, E. Yeatman, T. Green, and B. Stark, "Mems inertial power generators for biomedical applications," *Microsystem Technologies*, vol. 12, no. 10-11, pp. 1079–1083, 2006.

[31] E. M. Yeatman, P. D. Mitcheson, and A. S. Holmes, "Micro-engineered devices for motion energy harvesting," in *Electron Devices Meeting, 2007. IEDM 2007. IEEE International*. IEEE, 2007, pp. 375–378.

[32] "Warp wireless open-access research platform," https://mangocomm.com/products/kits/warp-v3-kit, 2017, accessed: 2017-08-25.

[33] C. T. Chou, A. Misra, and J. Qadir, "Low-latency broadcast in multirate wireless mesh networks," *IEEE Journal on Selected Areas in Communications*, vol. 24, no. 11, pp. 2081–2091, 2006.

[34] S. Sen, J. Xiong, R. Ghosh, and R. R. Choudhury, "Link layer multicasting with smart antennas: No client left behind," in *Network Protocols, 2008. ICNP 2008. IEEE International Conference on*. IEEE, 2008, pp. 53–62.

[35] "802.11 reference design for warp v3," https://warpproject.org/trac/wiki/802.11, 2018, accessed: 2018-09-29.

[36] C. Felini, M. Merenda, and F. G. D. Corte, "Dynamic impedance matching network for rf energy harvesting systems," in *2014 IEEE RFID Technology and Applications Conference (RFID-TA)*, Sept 2014.

[37] E. Rozner, V. Navda, R. Ramjee, and S. Rayanchu, "Napman: Network-assisted power management for wifi devices," in *Proceedings of the 8th International Conference on Mobile Systems, Applications, and Services*, ser. MobiSys '10. ACM, 2010.

[38] S. J. Chen, T. Kaufmann, and C. Fumeaux, "Wearable textile microstrip patch antenna for multiple ism band communications," in *2013 IEEE Antennas and Propagation Society International Symposium (APSURSI)*, July 2013.